SAND2013-0933C

Coupling of a Bladed Hub to the Tower of the Ampair 600 Wind Turbine

Experimental Substructuring using the Transmission Simulator Method

Daniel P. Rohe and Randy L. Mayes
Sandia National Laboratories†

† Sandia National Laboratories is a multi-program laboratory managed and operated by Sandia Corporation, a wholly owned subsidiary of Lockheed Martin Corporation, for the U.S. Department of Energy's National Nuclear Security Administration under contract DE-AC04-94AL85000.

Overview

- Introduction
- Substructuring Objectives
- Test Structures
  - Tower Model
  - Bladed Hub Model
- Substructuring Calculations
- Substructuring Results
- Error Sources
- Conclusions

Introduction: The Ampair 600 Test-Bed

- In the past few years a renewed interest in experimentally-based substructuring has developed.
- Groups interested in collaboration developed a test bed to enable sharing of techniques and results.
- Ampair 600 Turbine represents a ‘real-world’ application with joints, uncertain material properties, etc.

Sandia National Laboratories

Substructuring Objectives

- Derive experimental models for two substructures of the Ampair 600 assembly
- Couple these two models together using the Transmission Simulator method to predict the response of the assembly.

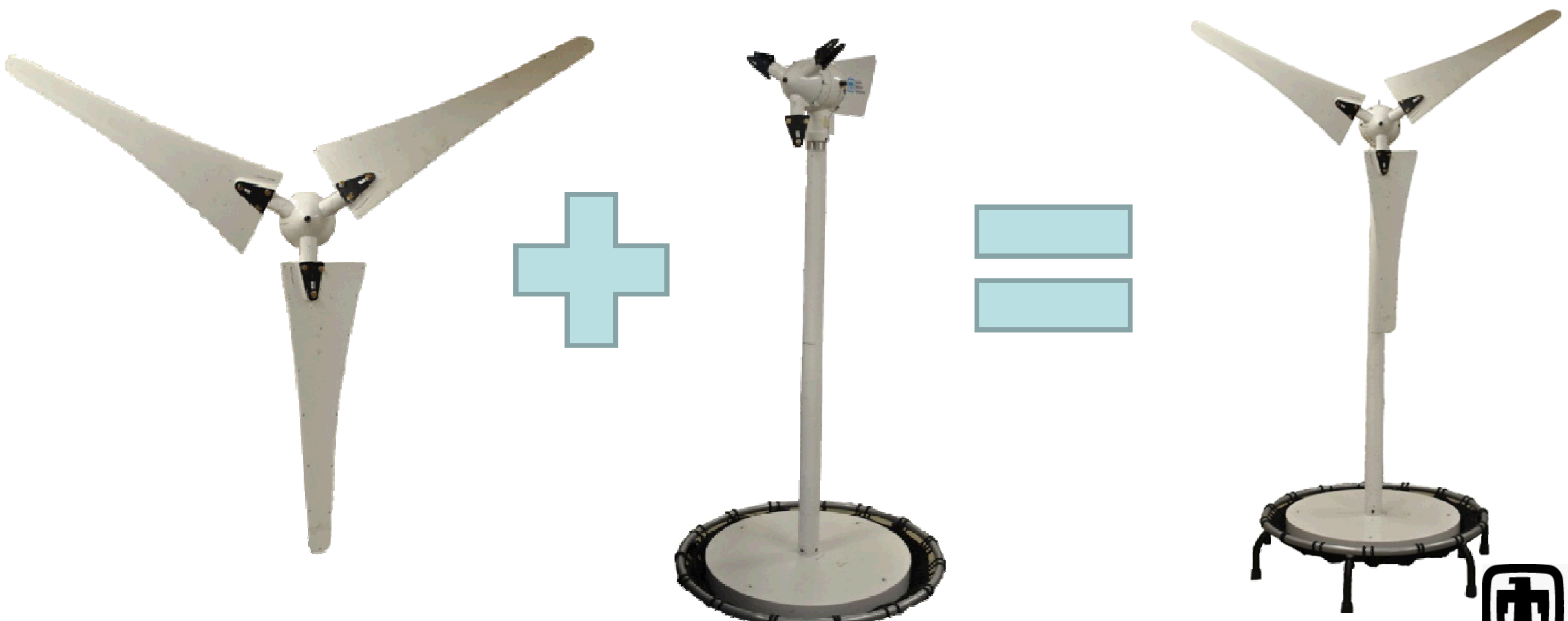

Sandia National Laboratories

Transmission Simulator Method Considerations

- Previous studies with the transmission simulator method have utilized a separate fixture as the transmission simulator.
- Save expense by using the hub as the transmission simulator
- Since a hub appears in both experimental sub-assemblies, one will need to be subtracted.

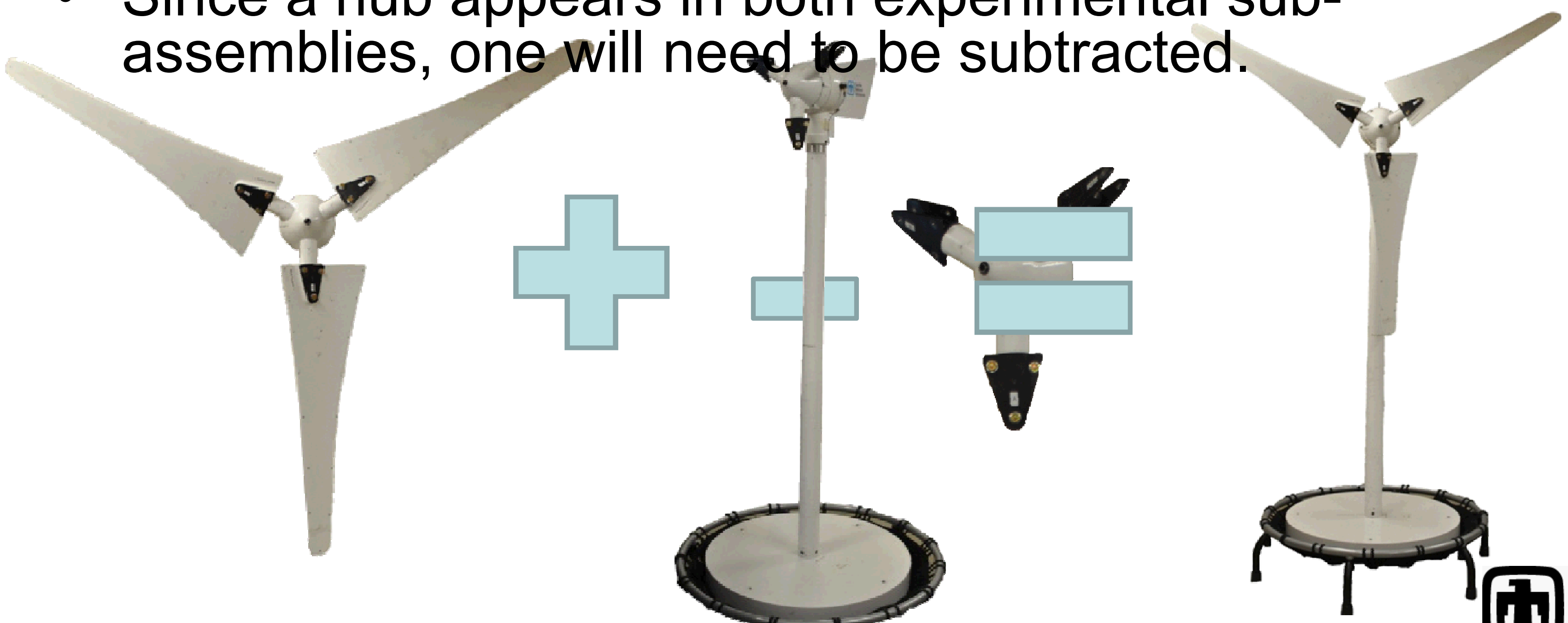

Sandia National Laboratories

Testing Parameters and Nomenclature

- Modes up to second bending of tower and blades (~100 Hz) of interest
- Test range from 0 to 156.25 Hz
- 0.3 kg (0.7 lb) impact hammer with softest available tip used to excite the structure
- Modes extracted with the SMAC algorithm

Bladed Hub Test

- Instrumented to distinguish first and second bending modes.
- Torsion modes not easily identifiable.
- Excited on hub and blade midpoints
  - Hitting blade tips gave large deformations and double-hits.

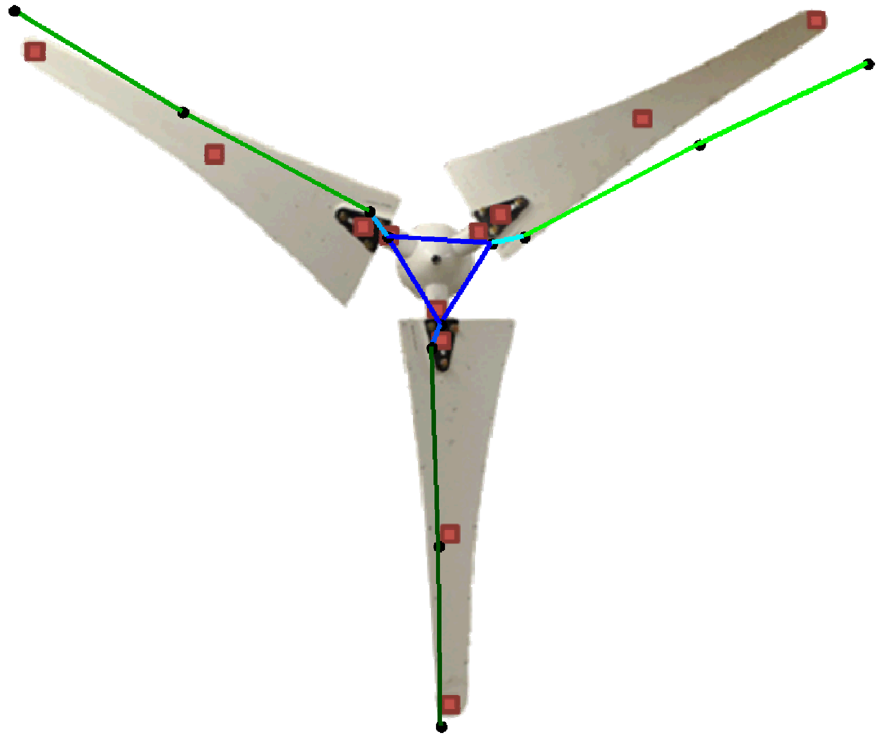

Bladed Hub Rigid Body Modes

- The bladed hub subassembly was supported on soft bungee cords
  - Approximate as free boundary
- Can analytically estimate rigid body modal parameters based on mass properties and geometry
- Hub mass properties measured with a Space Electronics mass properties machine
- Blade mass properties approximated from solid models
  - Uniform densities assigned to various portions of the blade
  - Densities calculated using total mass of blade and lengthwise center of gravity

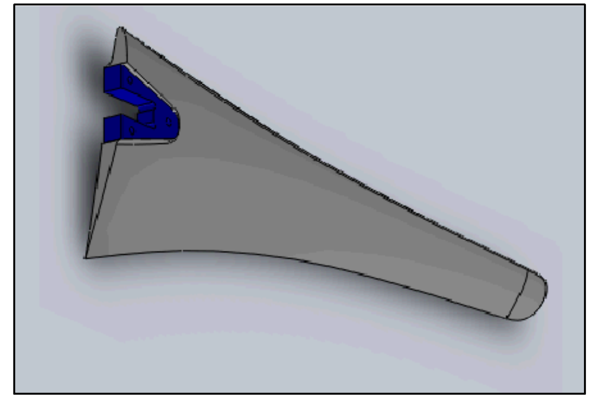

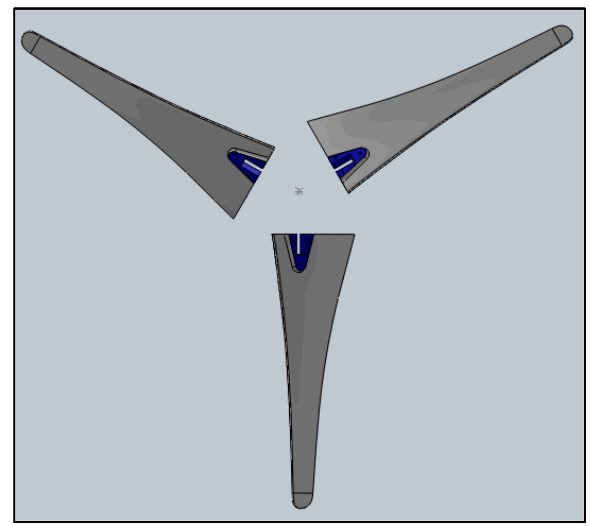

Blade Span: 940.5 kg/m^3
Blade Base: 2664.5 kg/m^3

Bladed Hub Results

- Created analytical rigid body modes at 0.1 Hz
- Modes extracted from 20.36 Hz to 153.1 Hz
- Peaks shift from reference to reference due to nonlinearities

Mode	Frequency (Hz)	Damping Ratio (%)	Description
1	0.1 *	0	x-direction Translation
2	0.1 *	0	y-direction Translation
3	0.1 *	0	z-direction Translation
4	0.1 *	0	Rigid Body Yaw
5	0.1 *	0	Rigid Body Pitch
6	0.1 *	0	Rigid Body Roll
7	20.36	2.17	1st Bending, 3 Blades in Phase
8	27.27	1.75	1st Bending, 1 Blade out of Phase
9	28.97	1.84	1st Bending, 1 Blade out of Phase
10	53.19	3.27	2 Blade Edgewise Mode
11	62.14	1.81	2 Blade Edgewise Mode
12	68.38	1.76	2nd Bending, 3 Blades in Phase
13	95.31	2.14	2nd Bending, 1 Blade out of Phase
14	100.05	1.50	2nd Bending, 1 Blade out of Phase

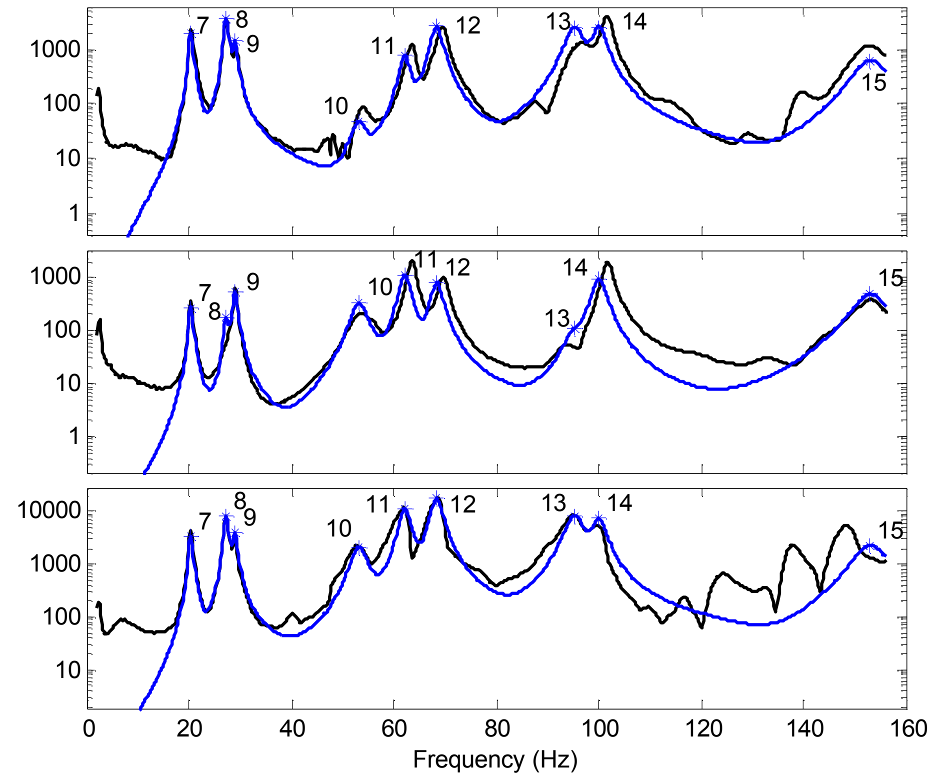

Top: z-direction on transmission simulator
Middle: θ-direction on transmission simulator
Bottom: z-direction on blade

Sandia National Laboratories

Bladeless Tower Test

- Instrumented to distinguish first and second tower modes
- High-sensitivity (500 mV/g) accelerometers used on massive base
- Excited a large number of drive points.
  - Tail, Pole, Hub Clamps, Hub Arms

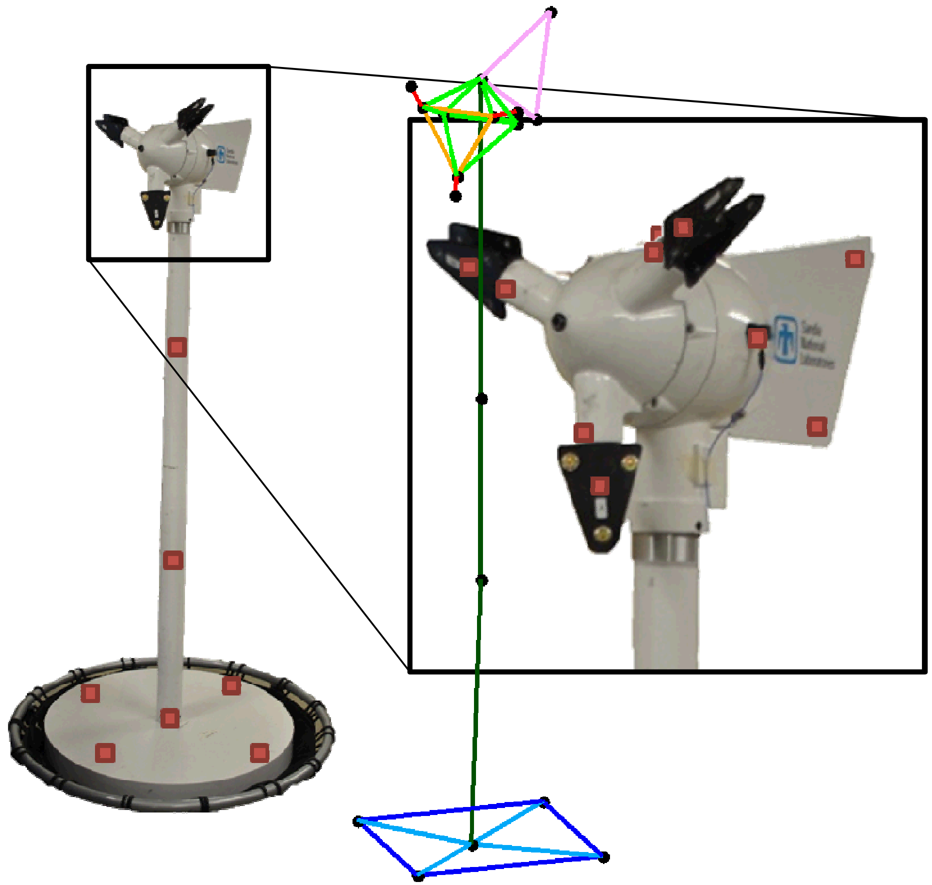

Tower Rigid Body Modes

- Tower rests on a modified commercial trampoline of unknown stiffness
- Highest 'rigid body' frequencies near 4 Hz
  - Lowest elastic frequencies near 20 Hz
  - Typically desire rigid body frequencies 10x lower than elastic frequencies for free boundary approximation
- *Accurate, properly-scaled rigid body modes are crucial to substructuring success!*

Measuring Tower Rigid Body Modes

- Used separate stepped-sine shaker test to extract rigid body modes.
- Tower drive points excite x- and z-direction translational modes and pitch and roll modes
- Base inputs excite y-direction (bounce) mode and yaw mode
- Rigid body mode shapes were a least-squares fit to the data of a linear sum of the analytical rigid body modes

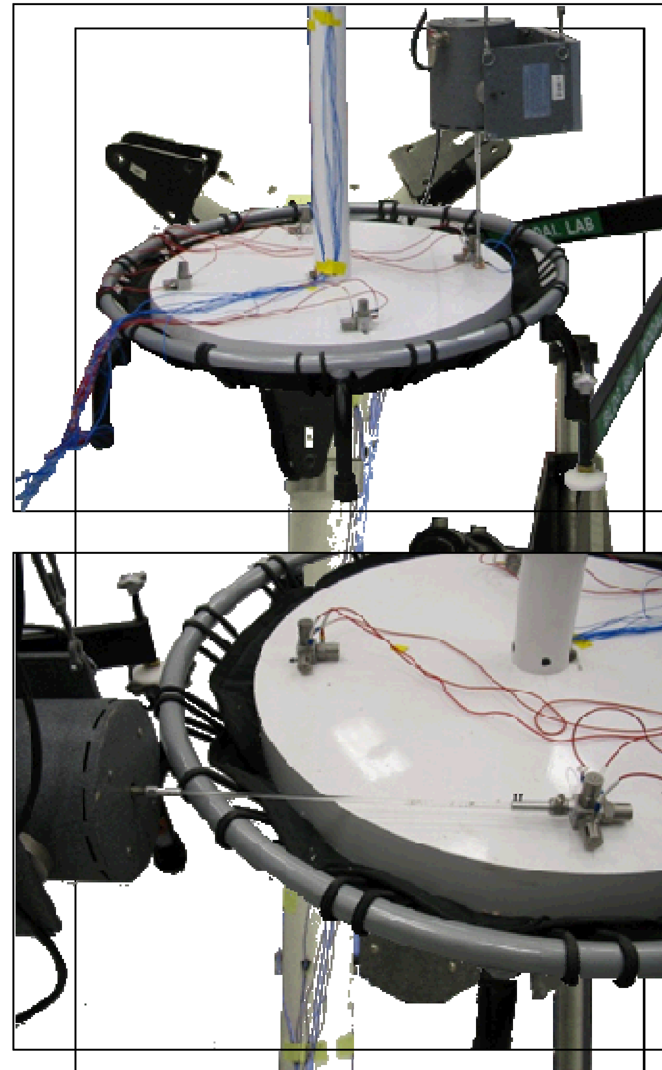

Tower Test Results

- Extracted modes from 0.89 Hz to 148.9 Hz.
- Data from tail drive points looked worse
  - Tail is relatively soft
  - Adequate force level gives large deformations, nonlinearities
- Extracted generator shaft torsion mode
  - Helps to characterize joint stiffness

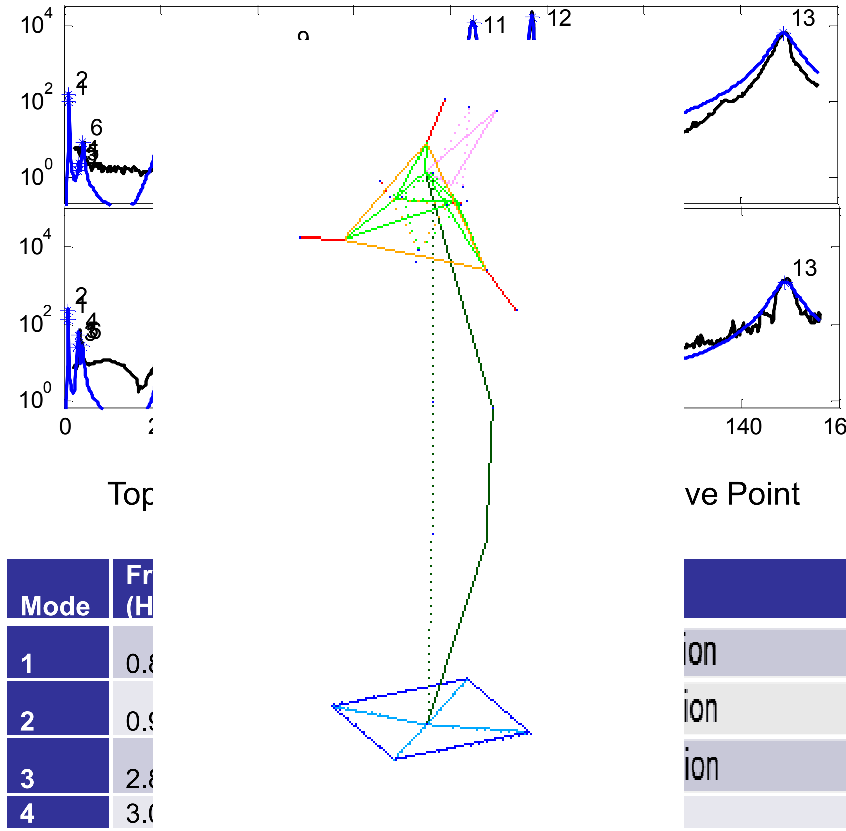

Mode	Fr (H		
1	0.8		ion
2	0.9		ion
3	2.8		ion
4	3.0		
5	3.25	6.57	Pitch Mode
6	3.93	6.69	Roll Mode
7	20.53	1.01	1st Bending in *yz*-plane
8	20.55	0.95	1st Bending in *xy*-plane
12	[illegible]	[illegible]	[illegible]
13	148.87	1.50	Generator Shaft Torsion
10	73.89	0.70	2nd Bending in *yz*-plane

Transmission Simulator

- A negative transmission simulator model is required to complete the substructuring calculations
- A simple tap test showed the first hub mode ~1200 Hz
- Transmission simulator assumed rigid
- Rigid body modes constructed from measured hub mass properties

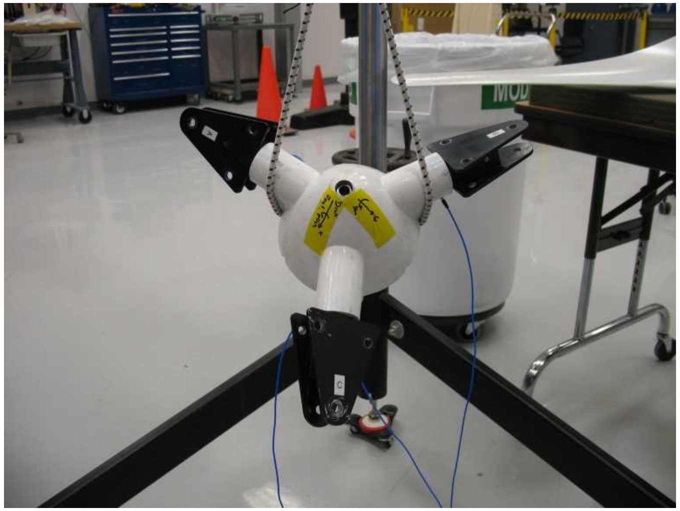

Sandia National Laboratories

Substructuring Calculations

- Transmission simulator method used to couple the two subassemblies as well as the *negative* transmission simulator model.

$$\begin{bmatrix} \mathbf{I}_t & & 0 \\ & \mathbf{I}_b & \\ 0 & & -\mathbf{I}_{TS} \end{bmatrix} \begin{Bmatrix} \ddot{\mathbf{q}}_t \\ \ddot{\mathbf{q}}_b \\ \ddot{\mathbf{q}}_{TS} \end{Bmatrix} + \begin{bmatrix} \left[\ddots 2\zeta_t\omega_t \ddots\right] & & 0 \\ & \left[\ddots 2\zeta_b\omega_b \ddots\right] & \\ 0 & & -\left[\ddots 2\zeta_{TS}\omega_{TS} \ddots\right] \end{bmatrix} \begin{Bmatrix} \dot{\mathbf{q}}_t \\ \dot{\mathbf{q}}_b \\ \dot{\mathbf{q}}_{TS} \end{Bmatrix} + \begin{bmatrix} \left[\ddots \omega_t^2 \ddots\right] & & 0 \\ & \left[\ddots \omega_b^2 \ddots\right] & \\ 0 & & -\left[\ddots \omega_{TS}^2 \ddots\right] \end{bmatrix} \begin{Bmatrix} \mathbf{q}_t \\ \mathbf{q}_b \\ \mathbf{q}_{TS} \end{Bmatrix} = \begin{Bmatrix} \mathbf{\Phi}_t^T \mathbf{F}_t \\ \mathbf{\Phi}_b^T \mathbf{F}_b \\ \mathbf{\Phi}_{TS}^T \mathbf{F}_{TS} \end{Bmatrix}$$

- Point-by-point constraints are assembled by equating motion on the hub of each subassembly with the motion of the transmission simulator

$$\begin{bmatrix} \mathbf{I} & 0 & -\mathbf{I} \\ 0 & \mathbf{I} & -\mathbf{I} \end{bmatrix} \begin{Bmatrix} \mathbf{x}_{t,m} \\ \mathbf{x}_{b,m} \\ \mathbf{x}_{TS,m} \end{Bmatrix} = \mathbf{0} \quad \text{or} \quad \begin{bmatrix} \mathbf{\Phi}_{t,m} & 0 & -\mathbf{\Phi}_{TS,m} \\ 0 & \mathbf{\Phi}_{b,m} & -\mathbf{\Phi}_{TS,m} \end{bmatrix} \begin{Bmatrix} \mathbf{q}_t \\ \mathbf{q}_b \\ \mathbf{q}_{TS} \end{Bmatrix} = \mathbf{0}$$

$$\boxed{\begin{aligned} \mathbf{x}_{t,m} &= \mathbf{x}_{TS,m} \\ \mathbf{x}_{b,m} &= \mathbf{x}_{TS,m} \end{aligned}}$$

Substructuring Methods, Continued

- Modal constraints are formed by pre-multiplying the point-by-point constraints by the pseudo-inverse of the transmission simulator mode shape matrices

$$\begin{bmatrix}\mathbf{\Phi}_{TS,m}^{+} & 0\\ 0 & \mathbf{\Phi}_{TS,m}^{+}\end{bmatrix}\begin{bmatrix}\mathbf{\Phi}_{t,m} & 0 & -\mathbf{\Phi}_{TS,m}\\ 0 & \mathbf{\Phi}_{b,m} & -\mathbf{\Phi}_{TS,m}\end{bmatrix}\begin{Bmatrix}\mathbf{q}_t\\ \mathbf{q}_b\\ \mathbf{q}_{TS}\end{Bmatrix}=\mathbf{B}\begin{Bmatrix}\mathbf{q}_t\\ \mathbf{q}_b\\ \mathbf{q}_{TS}\end{Bmatrix}=\mathbf{0}$$

$$\mathbf{\Phi}_{TS}^{+}\mathbf{x}_{t,m}=\mathbf{q}_{TS}$$
$$\mathbf{\Phi}_{TS}^{+}\mathbf{x}_{b,m}=\mathbf{q}_{TS}$$

- Transform into a coupled set of generalized coordinates $\mathbf{q}_u$ which account for the constrain equations

$$\begin{Bmatrix}\mathbf{q}_t\\ \mathbf{q}_b\\ \mathbf{q}_{TS}\end{Bmatrix}=\mathbf{L}\mathbf{q}_u$$

- Substitute

$$\mathbf{B}\mathbf{L}\mathbf{q}_u=0 \qquad\qquad \mathbf{L}=\mathrm{null}(\mathbf{B})$$

Substructuring Methods, Continued

- New equations of motion

$$\hat{\mathbf{M}}\ddot{\mathbf{q}}_u + \hat{\mathbf{C}}\dot{\mathbf{q}}_u + \hat{\mathbf{K}}\mathbf{q}_u = \mathbf{Q}$$

$$\hat{\mathbf{M}} = \mathbf{L}^T \begin{bmatrix} \mathbf{I}_t & & 0 \\ & \mathbf{I}_b & \\ 0 & & -\mathbf{I}_{TS} \end{bmatrix} \mathbf{L}$$

$$\hat{\mathbf{C}} = \mathbf{L}^T \begin{bmatrix} \begin{bmatrix} \ddots & & \\ & 2\zeta_t\omega_t & \\ & & \ddots \end{bmatrix} & & 0 \\ & \begin{bmatrix} \ddots & & \\ & 2\zeta_b\omega_b & \\ & & \ddots \end{bmatrix} & \\ 0 & & -\begin{bmatrix} \ddots & & \\ & 2\zeta_{TS}\omega_{TS} & \\ & & \ddots \end{bmatrix} \end{bmatrix} \mathbf{L}$$

$$\hat{\mathbf{K}} = \mathbf{L}^T \begin{bmatrix} \begin{bmatrix} \ddots & & \\ & \omega_t^2 & \\ & & \ddots \end{bmatrix} & & 0 \\ & \begin{bmatrix} \ddots & & \\ & \omega_b^2 & \\ & & \ddots \end{bmatrix} & \\ 0 & & -\begin{bmatrix} \ddots & & \\ & \omega_{TS}^2 & \\ & & \ddots \end{bmatrix} \end{bmatrix} \mathbf{L}$$

- Recover physical displacements

$$\mathbf{x} = \begin{bmatrix} \mathbf{\Phi}_t & & 0 \\ & \mathbf{\Phi}_b & \\ 0 & & \mathbf{\Phi}_{TS} \end{bmatrix} \mathbf{L}\mathbf{q}_u$$

Substructuring Results

- Substructured model compared to a truth test on the entire turbine.
- Good agreement for frequencies and mode shapes
- Average absolute damping error 36.8%

Truth Mode	Frequency (Hz)	Substr Match	Frequency (Hz)	Error	Truth Damping	Substr Damping	Error	MAC
Mode 1	17.24	Mode 1	17.86	3.58%	1.12%	0.99%	-12.08%	0.92
Mode 2	17.70	Mode 2	18.06	2.05%	0.78%	1.12%	44.53%	0.98
Mode 3	18.71	Mode 3	19.10	2.10%	0.81%	1.24%	52.68%	0.93
Mode 4	20.06	Mode 4	19.85	-1.02%	0.87%	1.32%	51.83%	0.97
Mode 5	21.46	Mode 5	21.21	-1.16%	0.92%	1.22%	32.93%	0.93
Mode 6	30.06	Mode 6	29.66	-1.32%	1.79%	0.44%	-75.37%	0.98
Mode 7	37.31	Mode 7	38.15	2.24%	1.00%	0.77%	-22.71%	0.99
Mode 8	48.38	Mode 8	51.27	5.98%	1.70%	2.65%	56.15%	0.62
Mode 9	54.87	Mode 9	56.92	3.74%	3.15%	1.40%	-55.52%	0.70
Mode 10	60.68	Mode 10	61.50	1.34%	1.96%	1.76%	-10.16%	0.83
Mode 11	66.16	Mode 11	66.31	0.21%	1.47%	1.70%	15.72%	0.72
Mode 12	68.60	Mode 12	75.41	9.93%	0.82%	0.77%	-6.58%	0.59
Mode 13	84.44	Mode 13	88.10	4.33%	0.92%	1.54%	66.43%	0.85
Mode 14	95.26	Mode 14	95.50	0.24%	1.14%	1.24%	9.15%	0.88
Mode 15	106.85	Mode 15	104.62	-2.09%	0.86%	0.92%	6.16%	0.93
Mode 16	121.28	-	-	-	1.15%	-	-	-
Mode 17	140.80	-	-	-	1.19%	-	-	-
Mode 18	149.85	Mode 16	152.36	1.68%	1.44%	2.47%	70.95%	0.83

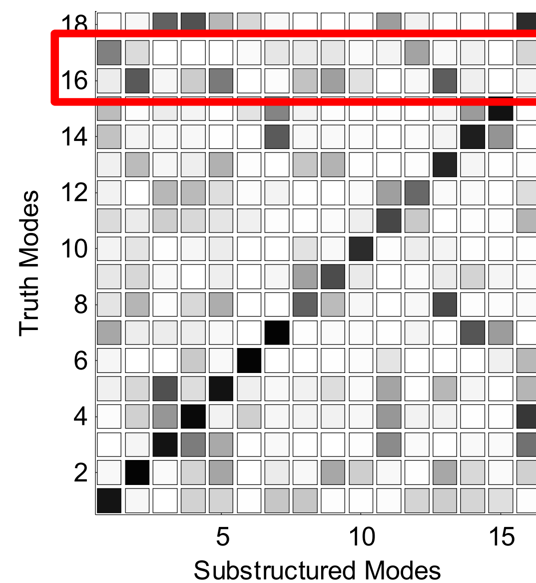

Sandia National Laboratories

Substructuring Results, Continued

- Low frequency mode shapes look good

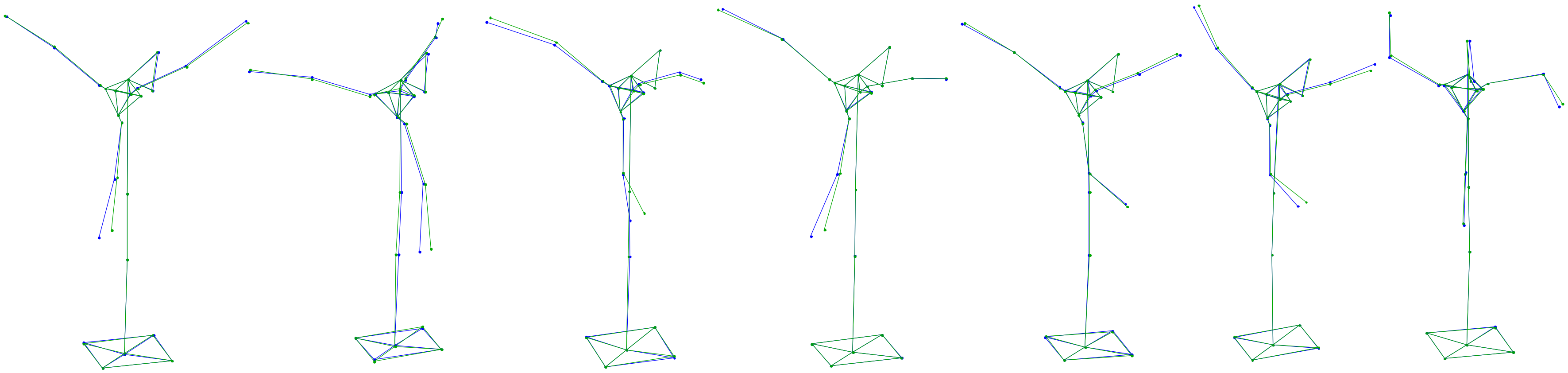

- Higher frequency mode shapes still bear visual resemblance

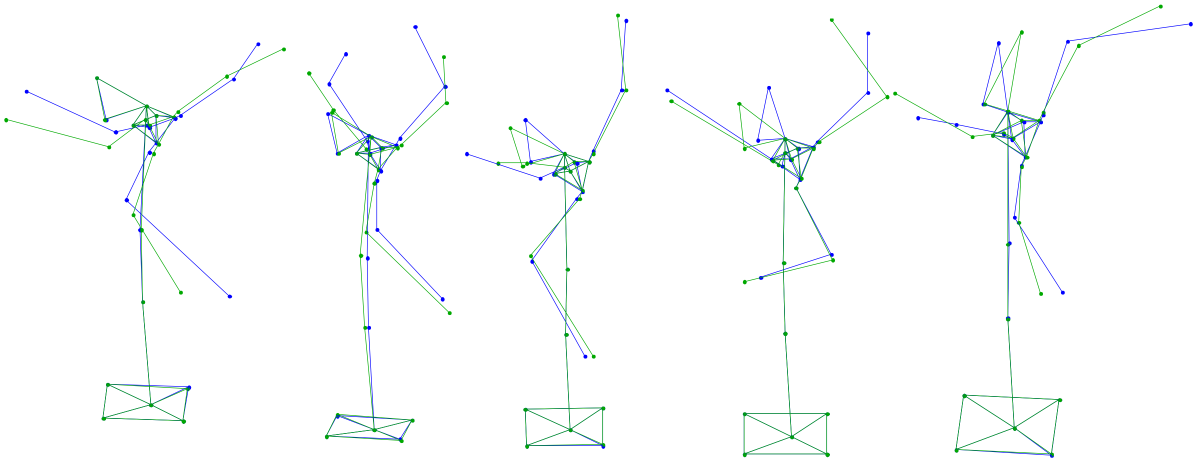

Substructuring Results, Continued

- CMIFs show frequency and scaling agreement

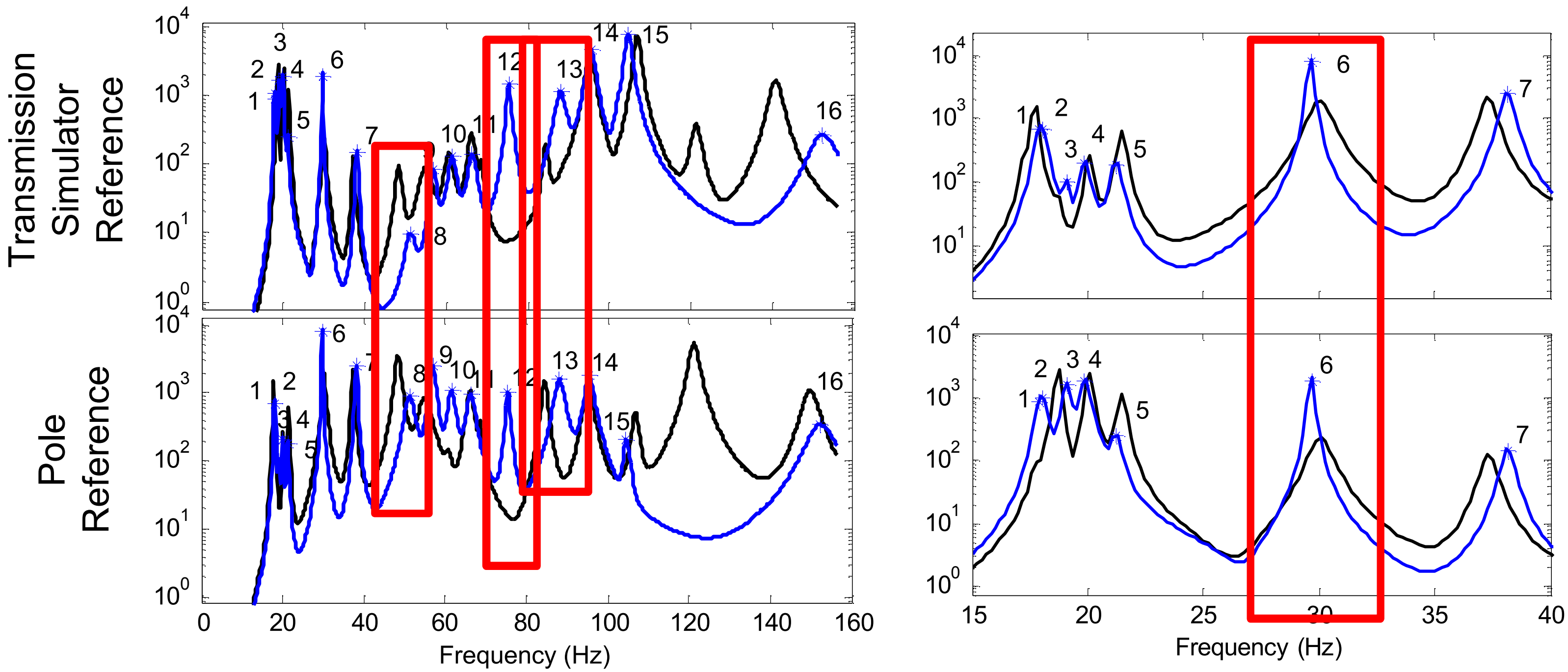

Some Possible Error Sources

- Rigid Body Mode Shape Scaling
  - Approximated mass properties based on solid model
  - Scale inertia properties to determine sensitivities
- Constraint Satisfaction
  - Transmission simulator doesn't enforce strict constraints
  - Rigid hub approximation is accurate
- Nonlinearity
  - Peaks shift between references
- Modal Truncation
  - Only one mode substantially above 100 Hz for each subassembly

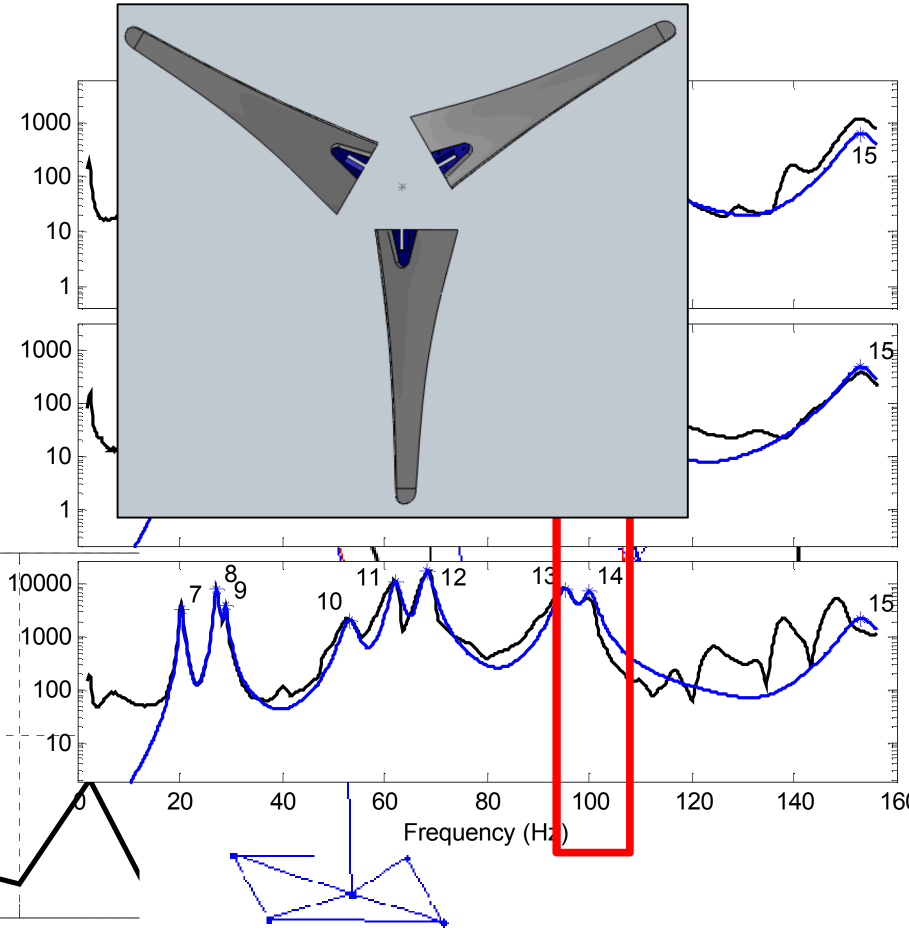

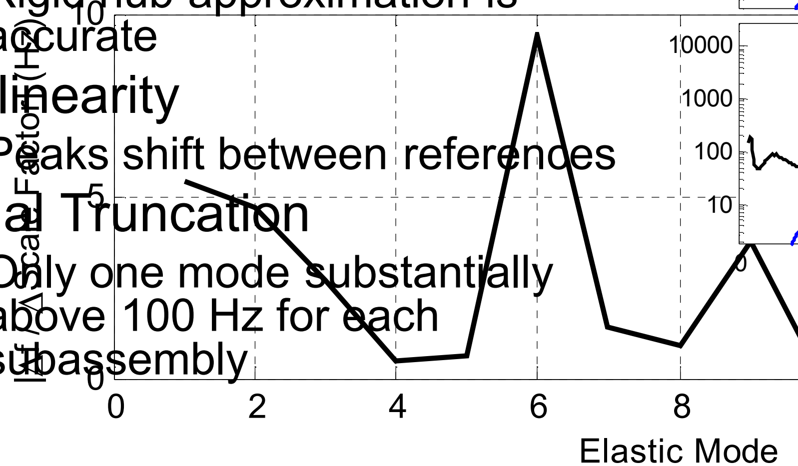

Conclusions

- Coupled experimental model of bladed hub to experimental model of bladeless tower
  - Both structures contain hub as transmission simulator
- Compared substructuring predictions with a truth test on the full turbine
- Substructuring predictions match truth data very well for first several modes:
  - Frequency errors < 3%
  - MAC > 0.90
- Higher frequency modes still have a good correlation
  - Two modes with frequency errors > 5%
  - Four modes with MAC < 0.8
- Damping not captured quite as well